ISBN: 978-3-95450-234-9 ISSN: 2673-5504 doi:10.18429/JACoW-SRF2023-MOPMB093

OPTIMIZING GROWTH OF NIOBIUM-3 TIN THROUGH PRE-NUCLEATION CHEMICAL TREATMENTS

S. Arnold*, L. Shpani†, G. Gaitan, M. Liepe, N. Sitaraman, Z. Sun
Cornell Laboratory for Accelerator-Based ScienceS and Education (CLASSE), Ithaca, NY, USA
T. Arias, Cornell University, Ithaca, NY, USA

Abstract

Niobium-3 tin is a promising alternative material for SRF cavities that is close to reaching practical applications. To date, one of the most effective growth methods for this material is vapor diffusion, yet further improvement is needed for Nb_3Sn to reach its full potential. The major issues faced by vapor diffusion are tin depleted regions and surface roughness, both of which lead to impaired performance. Literature has shown that the niobium surface oxide plays an important role in the binding of tin to niobium. In this study, we performed various chemical treatments on niobium samples pre-nucleation to enhance tin nucleation. We quantify the effect that these various treatments had through scanning electron microscopy and energy dispersive spectroscopy. These methods reveal information on tin nucleation density and uniformity, and a thin tin film present on most samples, even in the absence of nucleation sites. We present our findings from these surface characterization methods and introduce a framework for quantitatively comparing the samples. We plan to apply the most effective treatment to a cavity and conduct an RF test soon.

INTRODUCTION

Niobium-3 tin has great promise for applications in SRF cavities, with a higher critical temperature and the potential for more powerful acceleration in comparison to conventional niobium utilized in SRF particle accelerators. [1–11]. The state-of-the-art growth method of Nb_3Sn in SRF cavities is thermal vapor diffusion, which involves exposing a niobium cavity to vaporized tin and $SnCl_2$ to high temperatures in a high-temperature vacuum furnace. $SnCl_2$ has a higher vapor pressure than tin and is used as a nucleation agent at lower temperatures. While tin diffusion-based growth is the only method to date has consistently yielded high-performing Nb_3Sn cavities, there is still much room for improvement for this material to reach its theoretical limits. One key obstacle is achieving a consistently smooth and uniformly thick layer of stoichiometric Nb_3Sn, which is essential for high-performance, reliable cavities [2]. To address this challenge, this research focuses on optimizing the initial stage of this growth process, which involves the nucleation of tin-rich droplets on the oxide surface of the niobium substrate.

Past literature has shown the oxide present on the surface of niobium to be an active catalyst for various chemical processes, with some structures better suited to the binding of tin than others [12, 13]. Studies have shown that anodizing the niobium substrate prior to coating results in a more dense and uniform nucleation, as well as a smoother final Nb_3Sn film with smaller grains [2, 4]. This further confirms that oxygen plays a crucial role in the diffusion process. Additionally, DFT calculations suggest that acidic solutions which remove OH groups will generate more $SnCl_2$ binding sites, encouraging a more uniform nucleation [3, 14].

The goal of this study is to alter the niobium oxide through various chemical treatments with varying pH values, aiming to find an optimal treatment which will promote a uniform and dense distribution of tin nucleation sites on the niobium substrate, and thereby minimize the potential for surface roughness and tin depleted regions. This study presents a framework for and results of quantitatively comparing the impact of surface chemistry on the nucleation of tin and thin tin film formation on a niobium substrate.

EXPERIMENTAL METHOD

All samples were electropolished at room temperature and anodized prior to the application of the chemical treatments. Then, each sample, aside from the control, was soaked in prepared solutions for 30 minutes in a nitrogen atmosphere. The control sample had no additional chemical treatment applied after the anodization step. A photo of the samples (except the control) after soaking with labeled chemical treatments and respective pH value is shown in Fig. 1. After soaking, the samples were put in the vapor diffusion furnace for nucleation. For more details on the sample preparation, see Ref. [9]. The coating of the samples was halted after the nucleation step and samples were extracted for surface imaging and characterization.

The surface characterization techniques used are Scanning Electron Microscopy (SEM), and Energy Dispersive Spectroscopy (EDS). We analyzed the SEM images to characterize the formation of nucleation sites, also referenced to as droplets in this paper. EDS analysis of the samples was used to determine the atomic composition of the surface of the samples and to get information on the composition of the droplets, as well as to confirm thin tin film growth on each sample. For all EDS spectra, we used an accelerating voltage of 10 kV. By maintaining a constant accelerating voltage, we can obtain a relative comparison of the ratio of atomic compositions of Sn and Nb among our samples.

We used two types of EDS scans to attain the elemental composition of the samples: point analysis, and area scans. In point scans, the electron beam is focused on a chosen point on the sample, while in the area scans, the beam probes

* sga46@cornell.edu
† ls936@cornell.edu

ISBN: 978-3-95450-234-9 ISSN: 2673-5504 doi:10.18429/JACoW-SRF2023-MOPMB093

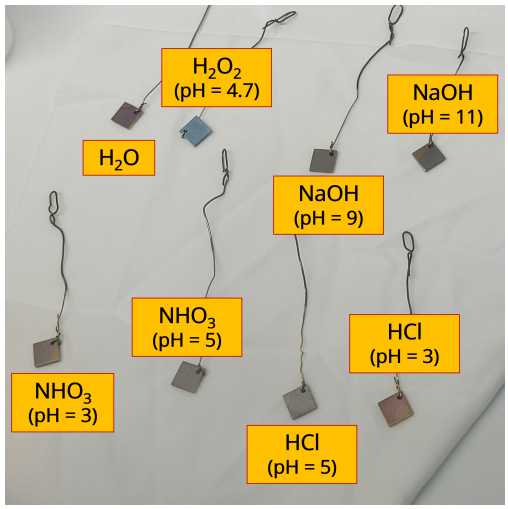

Figure 1: Samples after chemical treatments, before coating. From left to right, top to bottom the chemically treated samples are placed as water, H_2O, H_2O_2, NaOH (pH 11), NaOH (pH 9), NHO_3 (pH 3), NHO_3 (pH 5), HCl (pH 5), HCl (pH 3), with the control sample not shown [9].

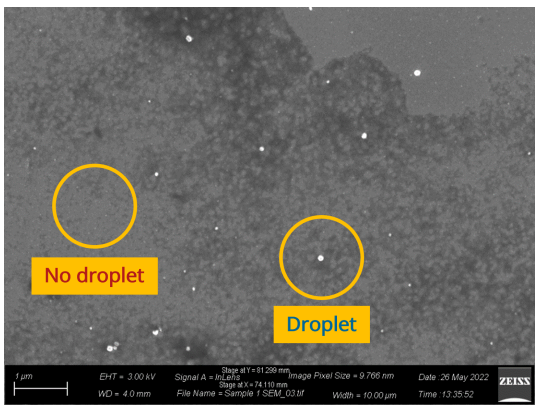

Figure 2: Circles illustrate roughly the area probed by point analysis scans on droplet and non-droplet areas on sample, shown on an SEM image.

larger (1800 μm^2 in our case) regions. Area scans are used to compare the overall composition of tin among our samples, sacrificing spatial resolution to achieve broader coverage.

While point analysis scans focus the electron beam in a sub-micron point on the surface of our samples, the probing area encompasses a roughly 1 µm radius region on our samples. With this type of scan, we were careful to find isolated nucleation sites that were further than a 1 µm radius to others. Similarly for the non-nucleation site (or "non-droplet") point analysis scans, we only probed areas that were at least 1 µm away from all other nucleation sites, to be able to relatively compare how much tin there is in individual droplets. This is illustrated in Fig. 2.

These two types of EDS analysis give information on the composition of the nucleation sites, the non-droplet areas where no nucleation sites were present, and the overall tin concentration on the samples.

RESULTS AND ANALYSIS

To identify potential tin depleted regions, we analyzed the uniformity of nucleated tin droplets on the surface of each sample and we compared the percentage of tin present on the non-droplet areas of each sample. We expect that many uniformly distributed tin-rich droplets, each within roughly a Nb_3Sn grain size distance of each other, will result in the desired smooth and stoichiometric Nb_3Sn.

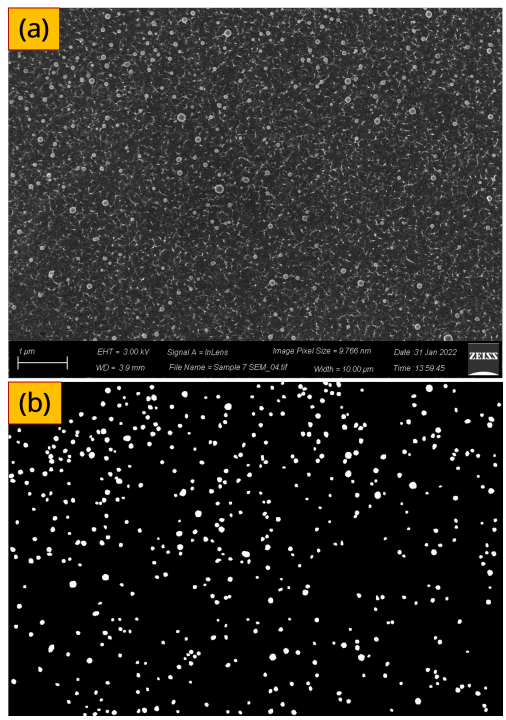

Figure 3: Example of SEM image pre- and post-processing with ImageJ Plugin StarDist. Here, StarDist identifies the white, circular nucleation sites, and converts the image into a mask which was further analyzed using other image processing methods [16, 17]. Original SEM image is pictured on the top (a), with the processed SEM image below (b).

SEM images of roughly 65 μm^2 areas were taken for each sample. The image processing software ImageJ was used to post-process the images and extract metrics about the distrubution of nucleation sites. More specifically, we used the plugin StarDist to identify the droplets on the surface [15–18]. Figure 3 shows an example of an SEM image pre (a) and post (b) processing. StarDist identifies the droplets and converts the image into a mask, which is further analyzed to extact the relevant metrics of interest. The average nearest neighbor calculation was done by utilizing the nearest neighbor ImageJ Macro.

Complementing the SEM analysis of the nucleation sites, EDS spectra of the samples were used to record a series of point and area spectra which were taken to analyze the atomic composition of the samples. This section outlines a procedure for quantitatively comparing the performance of samples, specifically in predicting tin depleted regions, and

ISBN: 978-3-95450-234-9 ISSN: 2673-5504 doi:10.18429/JACoW-SRF2023-MOPMB093

demonstrates that both SEM and EDS analysis of Nb_3Sn samples are necessary to determine the quality of nucleation.

SEM Uniformity Analysis

To determine the uniformity of each sample's nucleation sites, we first considered the density of nucleation sites. We analyzed the density of tin droplets over 16.25 μm^2 areas in SEM images. The second measure of uniformity of the nucleated droplets was the average distance from each particle to its six nearest neighbors. These metrics complemented each other, as the nearest neighbor calculations were susceptible to misrepresenting the uniformity of droplets due to clusters of six or more particles. Results from the density and average six nearest neighbor calculations are plotted together in Fig. 4.

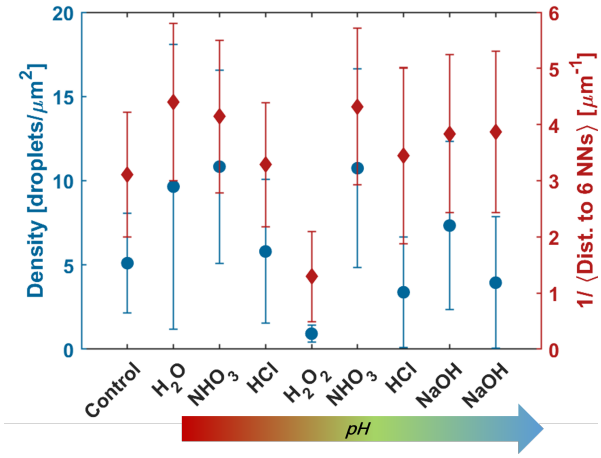

Figure 4: Comparative analysis of nucleation site density and inverse of average distance from six nearest neighbors of nucleated droplets for each treatment. Error bars represent one standard deviation from average values for both metrics and each sample.

Figure 4 highlights the non-uniform, sparse distribution of nucleation sites for the H_2O_2 treatment as compared to other samples, with the largest nearest neighbor distances and lowest density of particles. The samples treated by NHO_3, as well as the water treated sample have statistically higher densities and smaller average nearest neighbor distances than the other treatments.

The next set of analysis performed on the SEM images were tests to predict tin-depleted regions. Given that Nb_3Sn grains have a roughly 1 µm radius, a high quality coating is expected to have at least one nucleation site in every intended Nb_3Sn grain, i.e. 1 μm^2 area. To determine how each sample held up to this standard, we plot the number of times our average six nearest neighbor values and our density calculations allowed for droplets to be further apart than this maximum 1 µm radial distance in Fig. 5.

In this test, the NHO_3 with the lowest pH value and NaOH with the highest pH value stood out, both having no areas with density lower than 1 μm^{-2}. The NHO_3 treatments

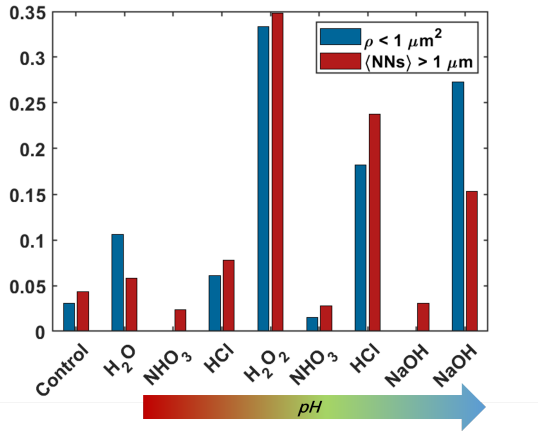

Figure 5: Normalized results from testing all average six nearest neighbor values and densities for tin depleted regions. The blue histogram (left) displays the normalized number of areas analyzed which have a density of under 1 nucleation site/μm^2, while the red histogram (right) shows the normalized number of nucleation sites with average six nearest neighbor distance greater than 1 µm.

had the lowest number of average distance to six nearest neighbors being bigger than 1 µm. As expected, H_2O_2 had the most predicted tin-depleted regions in both density and average distance to nearest neighbor values.

These results show that the type of chemical treatment has more of an impact on the quality of nucleation than the pH of that chemical treatment. NHO_3 with both pH values shows more promising results than HCl with the same low pH values. Furthermore, we see distinct performances between all treatments with pH values of 5, namely NHO_3, HCl and H_2O_2.

EDS Analysis

The goal of the EDS scans is to confirm that the droplets we see in the SEM images are indeed tin-rich, as well as to compare the relative tin content between our samples.

The results from the point analysis scans are shown in Fig. 6. We observed a high variation in tin concentration in the droplets imaged, which was not directly related to the size of the droplet. Furthermore, we observe a tin thin film present between the droplets in all treatments, except H_2O_2, which consistently showed no traces of tin when there were no droplets present.

The results from the area scans are shown in Fig. 7. The control sample demonstrated the highest overall tin content relative to the other samples. While this sounds promising for Nb_3Sn growth, the SEM images indicated clustering of nucleation sites. The lower pH treatments (HCl and NHO_3 with pH 3), and NaOH with pH 11 exhibit more tin than the treatments with pH values of 5. Finally, with a low density of droplets and no tin thin film present, H_2O_2 showed 0% tin on all the area scans as expected.

ISBN: 978-3-95450-234-9 ISSN: 2673-5504 doi:10.18429/JACoW-SRF2023-MOPMB093

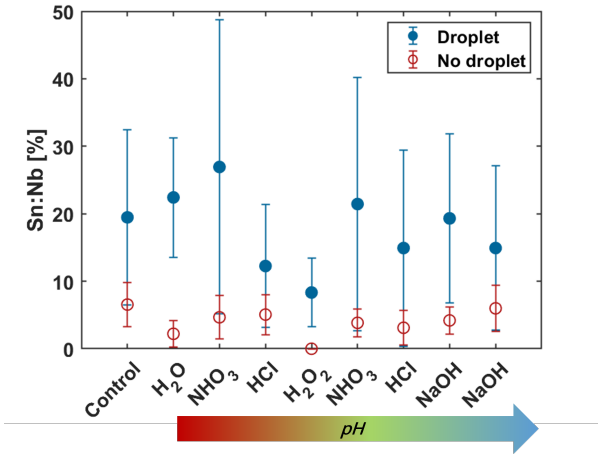

Figure 6: Ratio of atomic percentage of tin to niobium for droplet and non-droplet point analysis scans. Nucleation site areas are plotted in blue while non-nucleation site areas are plotted in red.

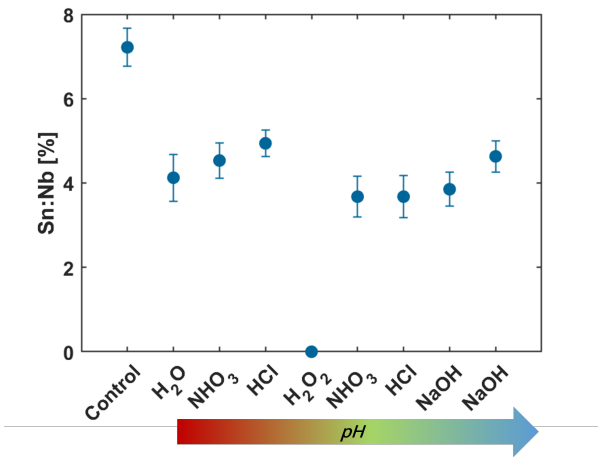

Figure 7: Ratio of atomic percentage of tin to niobium for larger (1800 μm^2) area EDS scans.

CONCLUSION

We conclude that chemical treatments of the niobium oxide influence the distribution of tin-rich droplets during the nucleation phase of vapor diffusion growth of Nb_3Sn. We found that the type of chemical treatment had a greater impact on the quality of nucleation compared to the pH of the treatment. H_2O_2 treatment showed the lowest density of droplets and lowest overall tin concentration, suggesting a significant suppression in nucleation. NHO_3 is a promising treatment to arise from this study with a dense and uniform distribution of nucleation sites, but other treatments such as NaOH are also viable options to explore further in the future. Another interesting observation is that the control sample, which was not soaked in any of the treatments post anodization, shows a less uniform nucleation of droplets and a significantly higher tin content compared to the sample which was soaked in H_2O post anodization.

It is clear that a combination of both surface imaging and elemental composition is necessary to gain information about the quality of nucleation. Seeing dense nucleation sites in the SEM imaging does not give us information about the tin present in between the droplets, which we have observed to vary from one treatment to another. On the other hand, a high tin content from an EDS area scan can correspond to clustered droplets, which we expect to result in a non-uniform growth and a rough surface of the final Nb_3Sn layer.

Future steps include performing another sample study for reproducibility, followed by a full coat to see how these nucleated tin-rich droplets and the tin thin film between them affect the final Nb_3Sn layer. Furthermore, we plan on applying our most promising treatment to a cavity and performing an RF test.

ACKNOWLEDGEMENTS

Work supported by the National Science Foundation under Grant No. PHY-1549132, the Center for Bright Beams. This work made use of the Cornell Center for Materials Research Shared Facilities which are supported through the NSF MRSEC program (DMR-1719875).

We would like to show our gratitude to M. Thompson for SEM and EDS training and help.

REFERENCES

[1] S. Posen and D. L. Hall, "Nb3Sn superconducting radiofrequency cavities: fabrication, results, properties, and prospects", *Supercond. Sci. Technol.*, vol. 30, p. 033004, 2017. doi:10.1088/1361-6668/30/3/033004

[2] R. D. Porter, "Advancing the maximum accelerating gradient of niobium-3 tin superconducting radiofrequency accelerator cavities: RF measurements, dynamic temperature mapping, and material growth", Ph.D. thesis, Phys, Dept., Cornell University, Ithaca, USA, 2021

[3] N. Sitaraman, "Theory work on SRF materials", Ph.D. thesis, Phys, Dept., Cornell University, Ithaca, USA, 2022

[4] D. Hall, "New insights into the limitations on the efficiency and achievable gradients in *Nb_3Sn* SRF cavities", Ph.D. thesis, Phys, Dept., Cornell University, Ithaca, USA, 2017.

[5] S. Posen, M. Liepe, and D. L. Hall, "Proof-of-principle demonstration of Nb3Sn superconducting radiofrequency cavities for high Q0 applications", *Appl. Phys. Lett.*, vol. 106, p. 082601, 2015. doi:10.1063/1.4913247

[6] S. Posen *et al.*, "Advances in Nb3Sn superconducting radiofrequency cavities towards first practical accelerator applications", *Supercond. Sci. Technol.*, vol. 34, p. 025007, 2021. doi:10.1088/1361-6668/abc7f7

[7] S. Posen and M. Liepe, "Advances in development of Nb3Sn superconducting radio-frequency cavities", *Phys. Rev. ST Accel. Beams*, vol. 110, p. 112001, 2014. doi:10.1103/PhysRevSTAB.17.112001

[8] K. Takahashi *et al.*, "First Nb3Sn Coating and Cavity Performance Result for High Efficiency Nb3Sn Cavity at KEK",

ISBN: 978-3-95450-234-9 ISSN: 2673-5504 doi:10.18429/JACoW-SRF2023-MOPMB093

in *Proc. Annual Meeting of Particle Accelerator Society of Japan*, QST-Takasaki Online, Japan, Aug. 2021, pp. 338–342.

[9] L. Shpani *et al.*, "Study of Chemical Treatments to Optimize Niobium-3 Tin Growth in the Nucleation Phase", in *Proc. IPAC'22*, Bangkok, Thailand, Jun. 2022, pp. 1295–1298. doi:10.18429/JACoW-IPAC2022-TUPOTK036

[10] U. Pudasaini, C. E. Reece, and J. K. Tiskumara, "Managing Sn-Supply to Tune Surface Characteristics of Vapor-Diffusion Coating of Nb3Sn", in *Proc. SRF'21*, East Lansing, MI, USA, Jun.-Jul. 2021, pp. 516–521. doi:10.18429/JACoW-SRF2021-TUPTEV013

[11] N. M. Verboncoeur, M. Liepe, R. D. Porter, and L. Shpani, "Next Generation SRF Cavities at Cornell University", in *Proc. IPAC'22*, Bangkok, Thailand, Jun. 2022, pp. 1303–1306. doi:10.18429/JACoW-IPAC2022-TUPOTK038

[12] Z. Sun *et al.*, "Reaction-based mechanism for Nb3Sn nucleation: Role of oxygen", 2023. doi:10.48550/arXiv.2305.05114

[13] K. Skrodczky *et al.*, "Niobium pentoxide nanomaterials with distorted structures as efficient acid catalysts", *Commun. Chem.*, vol. 2, p. 129, 2019. doi:10.1038/s42004-019-0231-3

[14] N. S. Sitaraman *et al.*, "New Recipes to Optimize the Niobium Oxide Surface From First-Principles Calculations", in *Proc. SRF'21*, East Lansing, MI, USA, Jun.-Jul. 2021. doi:10.18429/JACoW-SRF2021-TUPFDV010

[15] C. A. Schneider, W. S. Rasband, and K. W. Eliceiri "NIH Image to ImageJ: 25 years of image analysis", *Nat. Methods*, vol. 9, pp. 671–675, 2012. doi:10.1038/nmeth.2089

[16] U. Schmidt, M. Weigert, C. Broaddus, and G. Myers, "Cell Detection with Star-Convex Polygons", in *Proc. MICCAI 2018*, Granada, Spain, Sep. 2018, pp. 265–273. doi:10.1007/978-3-030-00934-2_30

[17] M. Weigert *et al.*, "Star-convex Polyhedra for 3D Object Detection and Segmentation in Microscopy", the *IEEE Winter Conferrence on Applications of Computer Vision (WACV)*, Mar. 2020. doi:10.1109/WACV45572.2020.9093435

[18] M. Haeri and M. Haeri, "Imagej plugin for analysis of scaffolds used in tissue engineering", *J. Open Res. Software*, vol. 3, Jan. 2015. doi:10.5334/jors.bn